

# Granite magma formation, transport and emplacement in the Earth's crust

N. Petford\*, A. R. Cruden†, K. J. W. McCaffrey‡ & J.-L. Vigneresse§

\* Centre for Earth and Environmental Science Research, Kingston University, Surrey KT1 2EE, UK

† Department of Geology, University of Toronto, Toronto, Ontario M5S 3B1, Canada

‡ Department of Geological Sciences, University of Durham, Durham, DH1 3LE, UK

§ CREGU, UMR 7566 CNRS, BP 23, 54501 Vandoeuvre Cedex, France

**The origin of granites was once a question solely for petrologists and geochemists. But in recent years a consensus has emerged that recognizes the essential role of deformation in the segregation, transport and emplacement of silica-rich melts in the continental crust. Accepted petrological models are being questioned, either because they require unrealistic rheological behaviours of rocks and magmas, or because they do not satisfactorily explain the available structural or geophysical data. Provided flow is continuous, mechanical considerations suggest that—far from being geologically sluggish—granite magmatism is a rapid, dynamic process operating at timescales of  $\leq 100,000$  years, irrespective of tectonic setting.**

**T**he Earth's granite crust harbours continental landmasses that have remained stable and above mean sea level for more than a billion years<sup>1</sup>. The withdrawal of large volumes of granitic magma from the deep continental crust and its emplacement at higher structural levels produces a dehydrated and refractory lower crust, and an upper crust enriched in felsic (iron- and silica-rich) minerals and heat-producing (radioactive) elements. This flux of siliceous melts from deeper levels has also concentrated many chemical elements important for life (including potassium, sodium, phosphorus, lithium and chlorine) close to the surface.

Continental granite magmatism involves four separate but potentially quantifiable stages—generation, segregation, ascent and emplacement<sup>2,3</sup>—that operate over length scales ranging from  $10^{-5}$  to  $10^6$  m. The nature of granite magmatism and associated continental growth has been investigated mostly through geochemical and isotope studies. But since the early 1990s, research into the origin of granite has shifted away from geochemistry towards understanding the underlying physical processes involved. As a result, dynamic models that operate on timescales of months to centuries are replacing the once-prevailing view of granitic magma production as a slow, equilibrium process that requires millions of years for completion.

Here we review the important physical processes that control how granitic melts are extracted from their source regions, transported through the Earth's crust and intruded (often with cumulative volumes in excess of  $4.5 \times 10^5$  km<sup>3</sup>) into pre-existing rock. Most granite plutons found in the upper continental crust seem to be emplaced as low-viscosity, crystal-poor ( $\leq 30\%$ ) magmas in tabular intrusions fed from depth by small magma batches that ascend rapidly, either in relatively thin conduits or channelled along shear zones. Space for the incoming magma is made by a combination of lateral and vertical displacements at moderate strain rates (typically  $>10^{-14}$  s<sup>-1</sup>) on timescales of less than 100,000 years.

## Partial melting of continental crust

Given the average thickness of the continental crust of about 35 km, typical geothermal gradients of  $20^\circ\text{C km}^{-1}$  do not generate temperatures high enough to melt common crustal rocks (generally more than  $800^\circ\text{C}$ )<sup>4</sup>. Although minor volumes ( $<25\%$ ) of partial melt can be produced by fluid-present melting at high water fugacity ( $a_{\text{H}_2\text{O}}$ ) during thermal relaxation of thickened orogens<sup>5</sup>, local melting is far more efficient where heat is advected into the crust from the underlying (hotter) mantle by basaltic magmas<sup>6,7</sup>.

Partial melting of crustal rocks pre-heated in this way is likely to be rapid, with models predicting a melt layer two-thirds the thickness of the basaltic intrusion forming in 200 years<sup>4,6</sup>, at a temperature of up to  $950^\circ\text{C}$ . Recent experiments on natural rock systems at temperatures comparable with those attained during basaltic underplating have shown the importance of reactions involving the breakdown of micas and amphiboles to produce melts of granitic composition under fluid-absent conditions (see refs 4 and 8 for a review). These reactions are characterized by steep, positive pressure–temperature slopes with most hydrous phases breaking down over a narrow temperature interval (about  $50\text{--}80^\circ\text{C}$ ), giving rise to melt fractions in the range 0.2–0.4 (Fig. 1). Compositional differences are reflected in higher melting temperatures<sup>9</sup>, with metapelites yielding 20% melt at around  $800^\circ\text{C}$ , whereas amphibolites require temperatures close to  $950^\circ\text{C}$  to generate similar amounts of melt. An important consequence of fluid-absent melting is the moderate to large positive volume change that accompanies some reactions<sup>10</sup>. For the case of crust heated from below, reaction-induced volume changes will lead to local fracturing and an accompanying reduction in rock strength caused by increased pore fluid (melt) pressures<sup>8,11</sup>. Deviatoric stress gradients can also develop in the vicinity of the intruding mafic heat source and promote local fracturing. These processes, in conjunction with regional tectonic strain, are important in providing enhanced fracture permeabilities of about  $10^{-10}\text{--}10^{-5}$  m<sup>2</sup> in the region of partial melting<sup>12</sup>, which aid subsequent melt segregation.

## Melt transport

Melt and magma (melt plus suspended solids) must be transported both within and out of the source region before final emplacement. The transport process operates on two length scales: segregation, marked by small-scale movement of melt (centimetres to decimetres), mostly within the source region, and long-range (kilometre-scale) ascent through the continental crust to the site of final emplacement.

**Segregation.** The ability of granitic melt to segregate mechanically from its matrix is strongly dependent on its physical properties, of which viscosity and density are the most important. The viscosity of silicate melt is a function of composition, temperature and water content<sup>13</sup>. For much of this century, granitic melt was commonly thought to have a viscosity close to that of solid rock<sup>14</sup>. However, recent experimental studies have found that granitic melts generated over a wide range of crustal pressure–temperature conditions have viscosities generally in the range  $10^8\text{--}10^3$  Pa s (refs

13–15). Figure 2 shows estimates of average melt viscosities calculated using models reviewed in ref. 15 for a typical tonalite ( $\text{SiO}_2$ , 65 wt%) and leucogranite ( $\text{SiO}_2$ , 75 wt%) as a function of the water content of the melt. The median viscosity ( $\eta$ ) of both liquids at their respective ‘ideal’ water contents of 4 and 6 wt% respectively is  $10^{3.8}$  and  $10^{4.9}$  Pa s, a difference of less than about 1.1  $\log_{10}$  units. An important implication of this material similarity is that those aspects of the segregation and ascent process moderated by the physical properties of the liquid should occur at broadly similar rates, regardless of tectonic setting and the pressure–temperature–time path of the protolith<sup>15</sup>.

Unlike the case in the mantle, where gravity-driven compaction can segregate basaltic melt over geologically reasonable timescales<sup>16,17</sup>, the higher viscosities of crustal melts limit compaction to length scales comparable with the mean grain size of the surrounding matrix<sup>17,18</sup>. Accordingly, most field evidence points to deformation as the dominant mechanism that segregates and focuses melt flow in the lower crust<sup>8,9</sup>, and possibly the upper mantle as well (for example, ref. 19). Rock deformation experiments on partially melted granite indicate that at melt fractions (porosities) of 10–40%, pore pressures converge on the mean stress or confining pressure, resulting in macroscopic deformation due to melt-enhanced embrittlement by cataclastic flow<sup>8,20,21</sup>. These experiments have challenged the long-standing notion of a fundamental rheological threshold (critical melt fraction) below which melt cannot be extracted (for example, ref. 22), and imply that deformation-enhanced segregation can in principle occur at any stage during partial melting<sup>8,20</sup>.

Mechanically derived melt segregation models have several important implications for geochemical models of granitic magmatism. First, as deformation-assisted melt segregation is efficient in moving melt in the range  $10^3 < \eta < 10^6$  from source to local sites of dilation on timescales of approximately  $10^{-1}$ – $10^4$  years<sup>20,23</sup>, melts may not attain chemical or isotopic equilibrium with their surrounding protolith before final extraction and ascent<sup>23,24</sup>. Second, the proven efficiency of melt segregation in a deformation field makes it unlikely that large, granitic magma chambers will form in the region of partial melting<sup>12,18</sup>.

**Ascent.** Gravity is still the most viable driving force for large-scale vertical transport of melt in the continental crust. However, the

traditional idea of buoyant granitic magma ascending through the continental crust as slow-rising, hot Stokes diapirs or by stoping has been largely replaced by models involving the ascent of granitic magmas in narrow conduits, either as self-propagating dykes<sup>10,25</sup>, along pre-existing faults<sup>26</sup> or as an interconnected network of active shear zones and dilational structures<sup>27,28</sup>. Although the case is still being made for diapiric ascent in the ductile lower crust<sup>29</sup>, the advantage of dyke/conduit ascent models is that they overcome the severe thermal and mechanical problems associated with transporting very large volumes of magma through the upper brittle continental crust<sup>30</sup>, as well as explaining the persistence of near-surface plutonism and associated silicic volcanism. However, it remains an open question as to whether plutons are fed by predominantly a few large conduits analogous to basaltic dykes found in ancient shield areas on Earth, dyke swarms similar to those associated with sea-floor spreading, or the pervasive flow of channelled magma<sup>31,32</sup>.

One of the most striking aspects of the ascent of granitic melt in dykes compared to diapiric rise is the extreme difference in magma ascent rate between both processes, with the former up to a factor of  $10^6$  faster depending upon the viscosity of the material and conduit width<sup>25,26</sup>. The narrow dyke widths ( $\sim 1$ – $50$  m) and rapid ascent velocities predicted by fluid dynamical models have found support in field and experimental studies<sup>33,34</sup>, while rheological models based on granular flow theory are helping to refine further the ascent rates of magmatic suspensions<sup>35</sup>. In contrast to diapiric ascent, chemical and thermal interaction between dyke magmas and surrounding country rock will be minimal, and there may be little evidence in the way of geological, geophysical or geochemical evidence to mark the passage of large volumes of granite magma through the crust<sup>10,25</sup>. Dyke ascent models also bring plutonic granite magmatism more in line with timescales characteristic of silicic volcanism and flood basalt magmatism. The latter provide an interesting corollary, where rapid emplacement at the surface is controlled by flow along deeply penetrating dykes that underlie plateau basalt provinces. These dykes are rarely exposed, but undoubtedly exist.

## Emplacement

The emplacement of granitic magma within the continental crust marks the final stage in the granite forming process. Emplacement is defined here as the switch from upward to horizontal flow, and is controlled by a combination of mechanical interactions (either

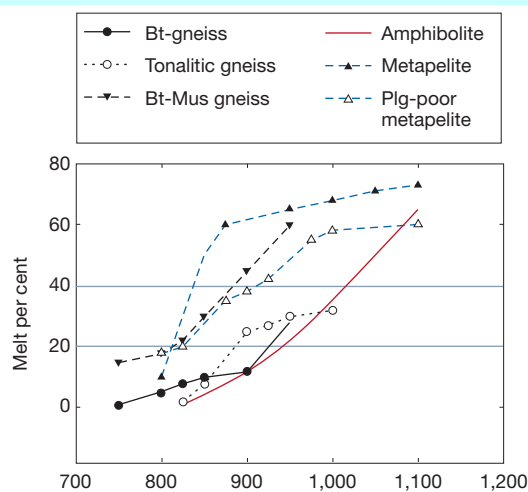


**Figure 1** Change in melt fraction (vol. %) as a function of temperature for a range of common crustal rock types undergoing fluid-absent melting (from ref. 9). Note the nonlinear increase in melt fraction with increasing temperature for all rock types. The amphibolite melting curve is a parametrization of seven experimental studies listed in refs 8, 18 and 25. The boxed area shows the range of melt fractions ( $F = 0.2$  to  $0.4$ ) required to produce most granite compositions. Bt-mus, biotite-muscovite; plg poor, plagioclase-poor; metapelite, metamorphosed pelite.

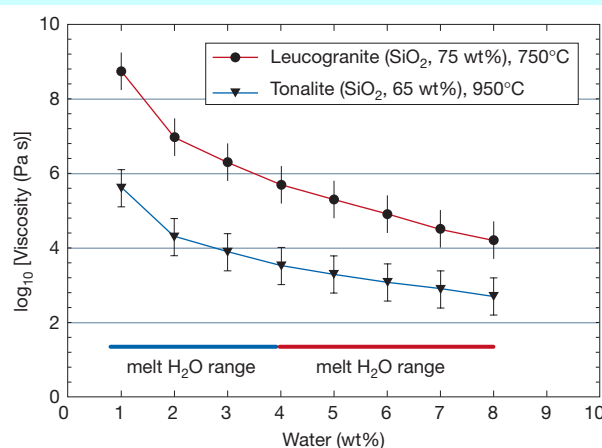
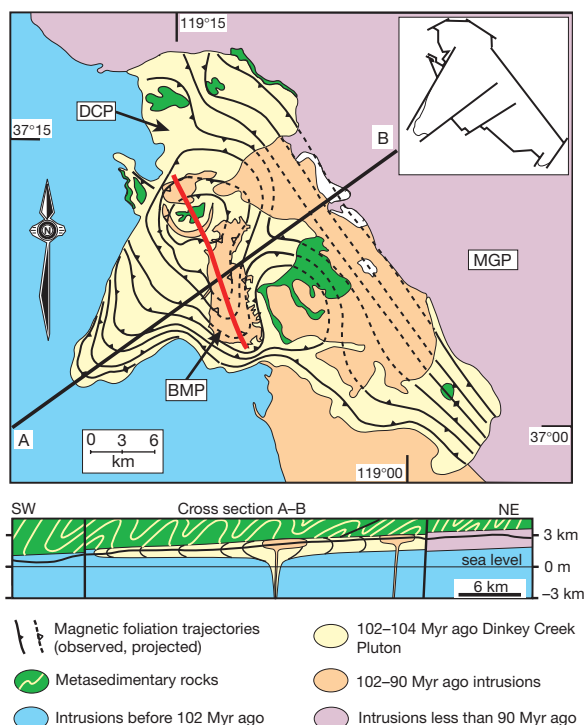


**Figure 2** Melt viscosity as a function of melt water (wt%) content for typical tonalite and leucogranite liquid compositions (data from ref. 15 and references therein) at a fixed pressure of 800 MPa. Blue and red horizontal lines show the range of water contents typical for natural melts. The estimated  $\log_{10}$  values of the median viscosities (in Pa s) of the liquids at their ‘ideal’ water contents of 4 wt% (tonalite) and 6 wt% (leucogranite) are 3.8 and 4.9 respectively.

pre-existing or emplacement-generated wall rock structures), and density effects between the spreading flow and its surroundings<sup>36,37</sup>. The way in which rocks make way for this newly incoming magma (the so-called space problem)<sup>14</sup> has challenged geologists for most of the twentieth century. The problem becomes particularly acute where batholithic volumes ( $\geq 1 \times 10^5 \text{ km}^3$ ) of magma are considered to have been emplaced in a single episode, often exemplified in models of diapiric rise, where the processes of ascent and emplacement are blurred<sup>25</sup>. New ideas that have helped improve this are the recognition of the important role played by tectonic activity in making space in the crust for incoming magmas (see ref. 37), more realistic interpretations of the geometry of granitic intrusions at depth (for example Box 1), and the recognition that

emplacement is an episodic processes involving discrete pulses of magma. Structural, analogue and numerical models<sup>38–41</sup> indicate that space for incoming magma at strain rates of between  $10^{-15}$  (average lithospheric strain rate) and  $10^{-10} \text{ s}^{-1}$  (several orders of magnitude greater than the average lithospheric strain rate) can be achieved through a combination of lateral fault opening, roof lifting and lowering of the growing magma chamber floor. In the latter two mechanisms, space is created ultimately by surface uplift and erosion or by volume reduction caused by melt extraction in the source<sup>40</sup>, possibly aided by isostatic depression of the Moho<sup>42</sup>. Such models resolve the insufficient strain record in the vicinity of certain plutons and the slow tectonic widening rates on bounding faults that have led some to question the ability of the crust to make space for incoming magma by fault dilation<sup>43</sup>.

#### Box 1



Geological map and cross section of the 800 km<sup>2</sup>, 102–104-Myr-old Dinkey Creek pluton, Sierra Nevada batholith, California. The pre-erosion thickness of the lobe structure in the southwest of the pluton is estimated to be between 900 and 3,700 m, based on fluid mechanical analysis of the magnetic fabric pattern, which also indicates a feeder zone trending to the north-northwest (red line on map)<sup>50,51</sup>. Evidence for a relatively flat roof above the pluton is provided by remnants of metasedimentary rocks preserved at high elevations. Structure contours on the contacts of these roof pendants indicate that the current roof dips about 10° SW. This is similar to the Cenozoic tilt of the adjacent Mount Givens pluton (MGP) determined by palaeomagnetic studies, suggesting that the Dinkey Creek pluton (DCP) roof was originally horizontal and located, on average, about 400 m above the present erosion surface. Geobarometry indicates that the pluton was emplaced at a palaeodepth of about 15 km (ref. 50). Repeated linear contact orientations, displacements of roof structure contours, and geometry of roof pendant contacts, suggest that the majority of the DCP's vertical contacts, and irregularities in its roof, were controlled by pre-existing NW-, NE-, N- and E-trending faults and fractures, which acted as guides for vertical displacement of the pluton floor (see inset). Similarly oriented structures controlled the shape of the 40 km<sup>2</sup> Bald Mountain pluton (BMP) and the 1,500 km<sup>2</sup> MGP.

#### Three-dimensional shapes of granitic intrusions

Important information on the emplacement mechanism of granitic magmas is preserved in the three-dimensional (3D) shape of the crystallized pluton. Detailed geophysical (gravity and seismic) data now allow the subsurface 3D geometries of granitic plutons to be imaged with a high degree of confidence. The majority of plutons so far investigated appear as flat-lying to open funnel-shaped structures with central or marginal feeder zones, consistent with an increasing number of field studies that find plutons to be internally sheeted on the decimetre to kilometre scale<sup>44</sup>. Gravity models based on detailed measurements made at the same spatial resolution as geological observations are now common. Depth determination, after gravity data inversion, structural measurements from field observations and determination of petrofabrics using the anisotropy of magnetic susceptibility (AMS) technique<sup>45</sup>, can be combined with geochemical information on magma evolution to build up a comprehensive 3D picture of pluton geometry<sup>46</sup>. Such multidisciplinary investigations again show that the common form is sheet-like as do the few detailed seismic surveys so far undertaken over or through granitic batholiths<sup>47</sup>.

#### Mechanism of pluton growth

Empirical studies of pluton dimensions, based on field and geophysical measurements, suggest that the growth of a laterally

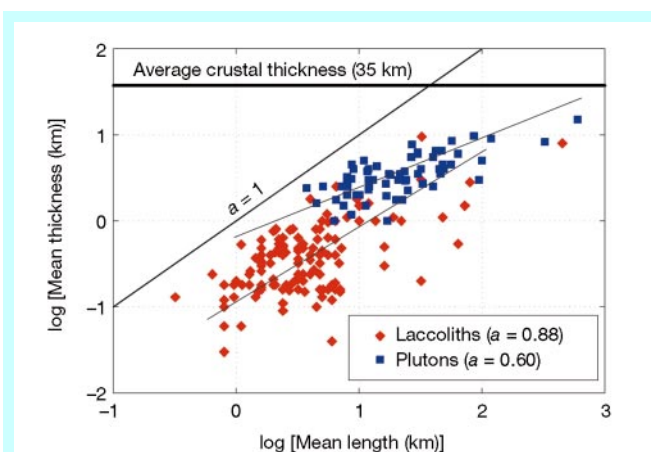


**Figure 3** Mean (vertical) thickness versus mean (horizontal) length for granitic plutons and laccoliths. Reduced major-axis regression defines a power-law curve for plutons with an exponent  $a$  of  $0.6 \pm 0.1$ . Laccoliths (shallow-level intrusions) are described by a power-law exponent of  $0.88 \pm 0.1$  (ref. 48). The line  $a = 1$  defines the critical divide between predominantly vertical inflation ( $a > 1$ ) and predominantly horizontal elongation ( $a < 1$ ) during intrusion growth. Significantly different power-law exponents rule out a simple genetic relationship between both populations. Differences may be due to mechanical effects, with limits in thickness reflecting floor depression (plutons) and roof lifting (laccoliths).

spreading and vertically thickening intrusive flow evolves according to a power-law (self-affine) relationship of the form  $L = kT^a$ , typical of systems exhibiting scale-invariant (fractal) behaviour<sup>48</sup>. The inherent preference for scale-invariant tabular sheet geometries in granitic plutons from a variety of tectonic settings is shown in Fig. 3. This relationship is best explained in mechanical terms by the need for magma at the emplacement level to travel horizontally some distance before vertical thickening can occur, either by hydraulic lifting of its overburden (in the case of shallow-level intrusions, known as laccoliths) or sagging of its floor. Plutons thus undergo a birth stage, characterized by lateral spreading, followed by an inflation stage marked by vertical thickening. Although from Fig. 3, plutons and laccoliths do not form a simple continuum as previously thought<sup>48</sup>, the tabular sheet model suggests that larger plutons grow from smaller ones according to a power-law inflation growth curve, ultimately to form crustal-scale batholithic intrusions<sup>40,48</sup>. Evidence of this growth process is recorded in the 1,200-km-long Coastal batholith of Peru, one of the best-studied arc batholiths on Earth. Here, combined field, petrological,

geochemical and geophysical (gravity) studies show that on a crustal scale the exposed batholith forms a thin (3–7-km-thick) low-density layer that coalesced from numerous smaller plutons with aspect ratios of between 17–20:1 (ref. 49). Detailed studies of the Sierra Nevada batholith of California reveal a similar picture, in which batholith construction occurred by intrusion of 2 to 2,000 km<sup>2</sup> granitic plutons between 120 and 80 Myr ago<sup>50</sup>. The Dinkey Creek pluton is typical of the intrusions that make up the central Sierra Nevada batholith (Box 1) and many other continental magmatic arcs. Field mapping of contacts, roof pendants and internal fabrics, combined with AMS studies, indicate that the pluton was emplaced as a 900–3,700-m-thick tabular intrusion with vertical walls and a gently dipping roof<sup>51</sup>. Magma was fed into the pluton by a conduit trending north-northwest, with space created by vertical inflation and depression of the floor caused by translation on pre-existing fractures in the wall rocks.

Timescales of pluton growth

The emerging picture of plutons, with tabular 3D geometry and growth by vertical displacements of their roofs and floors, allows us to place limits on the rates and times of their emplacement (Fig. 4). If we assume that a disk-shaped pluton grows according to the empirical power-law relation shown in Fig. 3

$$T = 0.6(\pm 0.15)L^{0.6\pm0.1} \tag{1}$$

then its filling time can be estimated when the volumetric filling rate,  $Q$ , is known. Taking conservative values of magma viscosities (Fig. 2), wall-rock/magma density differences and feeder dyke morphologies gives a range of  $Q$  from 0.01 to 100 m<sup>3</sup> s<sup>−1</sup>, and places lower and upper bounds on pluton filling times of less than 40 days to more than 1 Myr for plutons less than 1 km to more than 100 km across (Fig. 4). The thicknesses of the plutons highlighted in Box 1 have been estimated using the above power-law relationship, given the horizontal area and equivalent  $L$  value for each pluton. Taking the median  $Q$  value of 1 m<sup>3</sup> s<sup>−1</sup> gives ranges of net emplacement times of about 10<sup>3</sup>, 10<sup>4</sup> and 10<sup>5</sup> yr for the Bald Mountain, Dinkey Creek and Mount Givens plutons, respectively (Fig. 4). At the fastest magma delivery rates, all three plutons could have been emplaced in less than 1,000 yr. Similar timescales have been proposed for Himalayan granites<sup>52</sup>. We also note that the pluton thicknesses may have been over estimated by equation (1), as indicated by comparison to independent calculations of the thickness of the Dinkey Creek pluton lobe<sup>51</sup>, resulting in faster emplacement times for all three cases (Fig. 4).

Towards a unified model for granite magmatism

The formation of granite intrusions in the middle to upper crust is

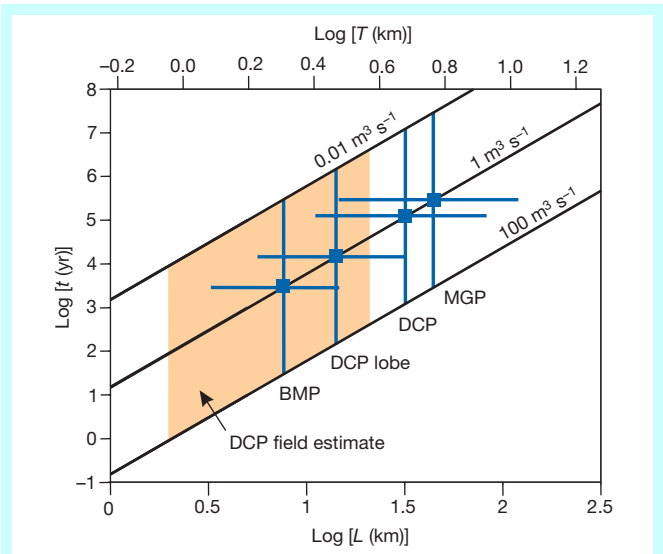


**Figure 4** Estimated filling times for tabular disk-shaped plutons. Their thickness ( $T$ ) to width ( $L$ ) ratio is given by equation (1) for a range of permissible filling rates ( $Q$ , m<sup>3</sup> s<sup>−1</sup>). Heavy horizontal lines are the thickness ranges of plutons in Box 1, estimated using equation (1). Vertical lines are the ranges of their possible filling times, bracketed by the filling rates. The coloured prism indicates the range of thicknesses estimated independently for the southwest lobe of the DCP using structural data (Box 1).

Table 1 The four processes responsible for granitic magmatism in the continental crust, and estimated timescales				
Process	Tectonic setting	Mechanism	Timescale (years)	References
<b>Partial melting</b>				
Fluid present (high $a_{\text{H}_2\text{O}}$ )	Transpressional/ transtensional orogens	Crustal thickening and decompression/ asthenospheric upwelling	$>10^5$	4, 5, 52
Fluid absent	Magmatic arcs (extensional/compressional)	Magmatic under/intraplating	$10^2\text{--}10^5$	4, 6, 7, 12
<b>Segregation</b>				
	Extensional/compressional	Gravity-driven compaction	$10^5\text{--}10^9$	16–18
		Deformation-enhanced flow/fracturing	$10^6\text{--}10^3$	16–18, 20, 21
<b>Ascent</b>				
Dyke/conduit flow	Mainly extensional	Buoyancy or deformation-assisted flow	$10^{-1}\text{--}10^2$	10, 25, 26, 34
Pervasive flow	Transpressional	Viscous flow in hot permeable crust	$\leq 10^6$	27, 28, 31, 32
Diapiric rise	Extensional/compressional	Buoyancy	$10^5\text{--}10^9$	29, 30, 43
<b>Emplacement</b>				
	Extensional/compressional	Entrainment along structural/ rheological traps, buoyancy	$10^2\text{--}10^4$	33, 36–40, 51, 52



governed by four discrete processes, summarized in Table 1. We have a number of reasons for confidence that these processes, running in series, provide an internally consistent qualitative model for granite magmatism in the Earth. First, field observations made in a variety of tectonic settings on rocks of different ages show that structural features relating to magma segregation, emplacement and pluton shape are repeated in space and time. We also find it encouraging that the high magma flow rates predicted in dyke ascent models can be reconciled with mechanical models for emplacement of tabular plutons at geologically realistic strain rates. Finally, tabular to funnel-shaped pluton geometries with inclined feeder zones predicted by fluid dynamical and structural models are consistent with recent high-resolution gravity and seismic investigations<sup>46</sup>. The rate-limiting step in granite magmatism is the timescale of partial melting<sup>3,52</sup>; the follow-on stages of segregation, ascent and emplacement can be geologically extremely rapid—perhaps even catastrophic.

Future experimental and numerical modelling of the underlying physics of each stage, and their associated feedback relations, will help to constrain further the rates at which these processes operate, and lead ultimately to models that capture the full complexity of granitic magma systems on the crustal scale. Problems yet to be tackled are numerous, and include matching predicted melting rates based on thermal models with kinetic studies of mineral reactions, and identification of a satisfactory focusing mechanism that enables partial melt distributed over a wide source region to be drained by a small number of conduits. □

1. Taylor, S. R. & McLennan, S. M. The geochemical evolution of the continental crust. *Rev. Geophys.* **33**, 241–265 (1995).
2. Brown, M. The generation, segregation, ascent and emplacement of granite magma: the migmatite-to-crustally-derived granite connection in thickened orogens. *Earth Sci. Rev.* **36**, 83–130 (1994).
3. Petford, N., Clemens, J. D. & Vigneresse, J. L. in *Granite: From Segregation of Melt to Emplacement* (eds Bouchez, J. L., Hutton, D. H. W. & Stephens, W. E.) 3–10 (Kluwer, Dordrecht, 1997).
4. Thompson, A. B. in *Understanding Granites: Integrating New and Classical Techniques* (eds Castro, A., Fernandez, C., Vigneresse, J. L.) 7–25 (Geological Society of London Special Publication 158, 1999).
5. Thompson, A. B. & Connolly, J. A. D. Melting of the continental crust: some thermal and petrological constraints on anatexis in continental collision zones and other tectonic settings. *J. Geophys. Res.* **100**, 15556–15579 (1995).
6. Huppert, H. E. & Sparks, R. S. J. The generation of granitic magmas by intrusion of basalt into continental crust. *J. Petrol.* **29**, 599–642 (1988).
7. Bergantz, G. W. Underplating and partial melting: implications for melt generation and extraction. *Science* **254**, 1039–1095 (1999).
8. Brown, M. & Rushmer, T. in *Deformation-Enhanced Fluid Transport in the Earth's Crust and Mantle* (ed. Holness, M.) 111–144 (Chapman & Hall, London, 1997).
9. Vigneresse, J. L., Barbey, P. & Cuney, M. Rheological transitions during partial melting and crystallisation with application to felsic magma segregation and transfer. *J. Petrol.* **37**, 1579–1600 (1996).
10. Clemens, J. D. & Mawer, C. K. Granitic magma transport by fracture propagation. *Tectonophysics* **204**, 339–360 (1992).
11. Watt, G. R., Oliver, N. H. S. & Griffin, B. J. Evidence for reaction-induced microfracturing in granulite facies migmatites. *Geology* **28**, 327–330 (2000).
12. Petford, N. & Koenders, M. A. Self-organisation and fracture connectivity in rapidly heated continental crust. *J. Struct. Geol.* **20**, 1425–1434 (1998).
13. Dingwell, D. B., Bagdassarov, N. S., Bussod, G. Y. & Webb, S. L. in *Experiments at High Pressure and Applications to the Earth's Mantle* (ed. Luth, R. W.) 131–196 (Short course Vol. 21, Mineralogical Association of Canada, 1993).
14. Pitcher, W. S. *The Nature and Origin of Granite* (Blackie Academic, Glasgow, 1993).
15. Clemens, J. D. & Petford, N. Granitic melt viscosity and silicic magma dynamics in contrasting tectonic settings. *J. Geol. Soc. Lond.* **156**, 1057–1060 (1999).
16. McKenzie, D. The generation and compaction of partially molten rocks. *J. Petrol.* **25**, 713–765 (1984).
17. Wickham, S. M. The segregation and emplacement of granitic magmas. *J. Geol. Soc. Lond.* **144**, 281–297 (1987).
18. Petford, N. Segregation of tonalitic-trondhjemitic melts in the continental crust: the mantle connection. *J. Geophys. Res.* **100**, 15735–15743 (1995).
19. Kelemen, P. B. & Dick, H. J. B. Focused flow and localized deformation in the upper mantle: juxtaposition of replacive dunite and ductile shear zones in the Josephine peridotite, SW Oregon. *J. Geophys. Res.* **100**, 423–438 (1995).
20. Rutter, E. H. & Neumann, D. H. K. Experimental deformation of partially molten Westerly granite under fluid-absent conditions with implications for the extraction of granitic magmas. *J. Geophys. Res.* **100**, 15697–15715 (1995).
21. Davidson, C., Schmid, S. M. & Hollister, L. S. Role of melt during deformation in the deep crust. *Terra Nova* **6**, 133–142 (1994).
22. Arzi, A. A. Critical phenomena in the rheology of partially molten rocks. *Tectonophysics* **44**, 173–184 (1979).
23. Sawyer, E. W. Disequilibrium melting and the rate of melt-residuum separation during migmatization of mafic rocks from the Grenville front, Quebec. *J. Petrol.* **32**, 701–38 (1991).
24. Davies, G. R. & Tommasini, S. Isotopic disequilibrium during rapid crustal anatexis: implications for petrogenetic studies of magmatic processes. *Chem. Geol.* **162**, 169–191 (2000).
25. Clemens, J. D., Petford, N. & Mawer, C. K. in *Deformation-Enhanced Fluid Transport in the Earth's Crust and Mantle* (ed. Holness, M.) 145–172 (Chapman & Hall, Lond. 1997).
26. Petford, N., Kerr, R. C. & Lister, J. R. Dike transport of granitoid magmas. *Geology* **21**, 845–848 (1993).
27. D'Lemos, R. S., Brown, M. & Strachan, R. A. Granite magma generation, ascent and emplacement within a transpressional orogen. *J. Geol. Soc. Lond.* **149**, 487–490 (1993).
28. Collins, W. J. & Sawyer, E. W. Pervasive granitoid magma transport through the lower-middle crust during non-coaxial compressional deformation. *J. Metamorph. Geol.* **14**, 565–579 (1996).
29. Weinberg, R. F. & Podladchikov, Y. Y. Diapiric ascent of magmas through power law crust and mantle. *J. Geophys. Res.* **99**, 9543–9559 (1994).
30. Marsh, B. D. On the mechanics of igneous diapirism, stoping and zone melting. *Am. J. Sci.* **282**, 808–855 (1982).
31. Brown, M. & Solar, G. S. The mechanism of ascent and emplacement of granite magma during transpression: a syntectonic granite paradigm. *Tectonophysics* **312**, 1–33 (1999).
32. Weinberg, R. F. Mesoscale pervasive felsic magma migration: alternatives to dyking. *Lithos* **46**, 393–410 (1999).
33. Scaillet, B., Pecher, A., Rochette, P. & Champenois, M. The Gangotri granite (Garhwal Himalaya): laccolith emplacement in an extending collisional belt. *J. Geophys. Res.* **100**, 585–607 (1994).
34. Brandon, A. D., Chacko, T. & Creaser, R. A. Constraints on rates of granitic magma transport from epidote dissolution kinetics. *Science* **271**, 1845–1848 (1996).
35. Petford, N. & Koenders, M. A. Granular flow and viscous fluctuations in low Bagnold number granitic magmas. *J. Geol. Soc. Lond.* **155**, 873–881 (1998).
36. Hogan, J. P. & Gilbert, M. C. The A-type Mount Scott granite sheet: importance of crustal magma traps. *J. Geophys. Res.* **100**, 15799–15792 (1995).
37. Hutton, D. H. W. Granite emplacement mechanisms and tectonic controls: inferences from deformation studies. *Trans. R. Soc. Edinb.: Earth Sci.* **79**, 245–255 (1988).
38. Fernandez, C. & Castro, A. Pluton accommodation at high strain rates in the upper continental crust. The example of the Central Extremadura batholith, Spain. *J. Struct. Geol.* **21**, 1143–1149 (1999).
39. Benn, K., Odonne, F. & de Saint Blanquat, M. Pluton emplacement during transpression in brittle crust: new views from analogue experiments. *Geology* **26**, 1079–1082 (1998).
40. Cruden, A. R. On the emplacement of tabular granites. *J. Geol. Soc. Lond.* **155**, 853–862 (1998).
41. Roman-Berdiel, T., Gapais, D. & Brun, J. P. Granite intrusion along strike-slip zones in experiment and nature. *Am. J. Sci.* **297**, 651–678 (1997).
42. Brown, E. H. & McClelland, W. C. Pluton emplacement by sheeting and vertical ballooning in part of the southeast Coast Plutonic Complex, British Columbia. *Geol. Soc. Am. Bull.* **112**, 708–719 (2000).
43. Miller, R. B. & Paterson, S. R. In defence of magmatic diapirs. *J. Struct. Geol.* **21**, 1161–1173 (1999).
44. Grocott, J., Garde, A., Chadwick, B., Cruden, A. R. & Swager, C. Emplacement of Rapakivi granite and syenite by floor depression and roof uplift in the Paleoproterozoic Ketildian orogen, South Greenland. *J. Geol. Soc. Lond.* **156**, 15–24 (1999).
45. Bouchez, J. L., Hutton, D. H. W. & Stephens, W. E. (eds) *Granite: From Segregation of Melt to Emplacement* (Kluwer, Dordrecht, 1997).
46. Améglio, L. & Vigneresse, J. L. in *Understanding Granites: Integrating New and Classical Techniques* (eds Castro, A., Fernandez, C., Vigneresse, J. L.) 39–54 (Geological Society of London Special Publication 158, 1999).
47. Evans, D. J. et al. Seismic reflection data and the internal structure of the Lake District batholith, Cumbria, northern England. *Proc. Yorkshire Geol. Soc.* **50**, 11–24 (1994).
48. McCaffrey, K. J. W. & Petford, N. Are granitic intrusions scale invariant? *J. Geol. Soc. Lond.* **154**, 1–4 (1997).
49. Atherton, M. P. Shape and intrusion style of the Coastal batholith, Peru. In *4th Int. Symp. on Andean Geodynamics* (extended abstr.) 60–63 (1999).
50. Bateman, P. C. Plutonism in the central part of the Sierra Nevada batholith, California. *US Geol. Surv. Prof. Pap.* **1483** (1992).
51. Cruden, A. R., Tobisch, O. T. & Launeau, P. Magnetic fabric evidence for conduit-fed emplacement of a tabular intrusion: Dinkley Creek pluton, central Sierra Nevada batholith, California. *J. Geophys. Res.* **104**, 10511–10530 (1999).
52. Harris, N., Vance, D. & Ayres, M. From sediment to granite: timescales of anatexis in the upper crust. *Chem. Geol.* **162**, 155–167 (2000).

## Acknowledgements

We would like to thank M. Brown and A. Brandon for helpful reviews and J. Clemens and M. Atherton for useful discussions during the preparation of this manuscript.

Correspondence and requests for materials should be addressed to N.P. (e-mail: n.pet@kingston.ac.uk).